



Electrochemical promotion for hydrogen production via ethanol steam reforming reaction

Estela Ruiz López, Fernando Dorado, Antonio de Lucas-Consuegra*

Department of Chemical Engineering, School of Chemical Sciences and Technologies, University of Castilla-La Mancha, Avenida Camilo José Cela 12, 13005 Ciudad Real, Spain



ARTICLE INFO

Keywords:

Electrochemical promotion
Ethanol reforming
Hydrogen production
Carbon deposition
Catalyst regeneration

ABSTRACT

In this work we have investigated for the first time the electrochemical activation of a catalyst for the ethanol reforming reaction. For that purpose, a Pt-K β Al₂O₃ electrochemical catalyst has been prepared, characterized and tested under ethanol reforming reaction conditions. The electrochemically supply of potassium ions under negative polarization step, strongly increased the hydrogen production rates leading to a reversible and controllable promotional effect. It has been attributed to the enhancement of the kinetic of ethanol dehydrogenation reaction, due to the strengthening of the chemisorptive bond of intermediate ethoxy molecules. It will increase the stability of this intermediate, thus favoring its formation, which initiates the ethanol reforming process. However, a large amount of carbonaceous species were formed on the catalyst surface during the negative polarization step that causes a continuous decrease in the catalytic activity under long polarization times. Under these conditions, the application of a catalyst potential of 2 V leads to a complete removal of the previous deposited carbonaceous molecules which allows further electrochemical activation steps. The obtained catalytic results have been supported by in-situ temperature programmed oxidation analysis and ex-situ Raman spectroscopy and Scanning Electron Microscopy. These techniques, in conjunction with the obtained catalytic results, have demonstrated the interest of the EPOC phenomenon for in-situ tuning the adsorption of reactants molecules on catalyst surface and its application in the hydrogen production technology, improving catalyst conversion and selectivity.

1. Introduction

The search for sustainable energy systems has encouraged, among several alternatives, the development of hydrogen-based technologies to reduce the impact of non-renewable sources. In fact, hydrogen, although it is not found in its elemental form, is the most abundant element on the world and possesses the highest specific energy content of all conventional fuels [1]. In order to not increase the amount of greenhouse gases, the utilization of biomass derived material such as alcohols is one of the promising solutions for the hydrogen production.

Ethanol steam reforming (ESR) has become an attractive route for hydrogen production, attending to the overall stoichiometric equation:



Ethanol, compared to other molecules like methanol or dimethyl ether, offers many favorable features such as safety in storage, handling and transportation, lack of toxicity, lower volatility, high hydrogen content and availability from renewable resources [2,3]. These

features, joint to their chemical energy, favor the use of ethanol for hydrogen production through different technologies including partial oxidation, dry and steam reforming or autothermal reforming [4,5].

Consequently, catalytic steam reforming has been widely studied using different types of catalysts and support materials. Noble metals (Au, Pd, Pt, Rh, Ru) [6–9] and transient metals (Co, Cu, Ni) [5,10–13] catalysts have been tested, as well as combinations between them, creating bimetallic [3,14,15] catalysts. These metallic catalysts have been supported on different materials, such as SiO₂, CeO₂, Al₂O₃, Ce_{0.6}Zr_{0.4}O₂, Nb₂O₅, ZnO, HAp [16–19]. Different studies [14,17,20,21] have also used different kind of promoters to enhance the catalytic activity by adding species to the catalytic active phase. However, and despite all efforts made, there are currently no available commercial catalyst to ethanol steam reforming [22]. The development of an efficient catalyst, capable of overcoming by-product formation, catalytic deactivation [23], and the continuous heat supply (due to the strongly endothermic behaviour) [24] is one of the main remained challenges [25].

* Corresponding author.

E-mail address: Antonio.lconsuegra@uclm.es (A. de Lucas-Consuegra).

The phenomenon of electrochemical promotion of catalysis (EPOC), also known as non-faradaic electrochemical modification of catalytic activity (NEMCA), discovered by Stoukides and Vayenas in 1981 [26], has recently shown to be an alternative way to promote and enhance catalytic reaction rates. It is based on the activation of a catalyst by the electrochemical supply of promoter ions from an electro-active catalyst support (solid electrolyte) by means of the application of electrical polarizations on a solid electrolyte cell. Hence, the electrochemical promotion phenomenon allows to control in a continuous and reversible manner the in-situ addition or removal of promoters to the catalyst under reaction conditions. This effect makes possible a fast and precise evaluation and optimization of the promoter coverage on the catalyst surface [27]. Additionally, on the last years this phenomenon has been shown to be a useful tool to modify the reversible oxidation state of a catalyst [28,29], to prevent poisoning effects [30] or even to regenerate the catalyst from carbon deposition during the course of the catalytic reaction [31].

The application of the EPOC phenomenon in hydrogen production reactions has been already studied in different catalytic systems. For instance, it has been studied on the water-gas shift (WGS) reaction using Pt as catalyst and yttria-stabilized zirconia (YSZ, O²⁻ conductor) [32] as solid electrolyte, and Ni supported on K-βAl₂O₃ (K⁺ conductor) [33]. The methane steam reforming reaction has also been studied on Ni and Pt, both supported over YSZ solid electrolyte [34,35]. On the other hand the EPOC effect has also been studied on the steam reforming of methanol using Ni and Cu supported over K-βAl₂O₃ [30,36]. All these studies have shown a great interest of the application of EPOC phenomenon in the hydrogen production technology with a great significance and many interesting issues which have recently been reviewed in a recent work [37].

The aim of the present work is to investigate for the first time in literature, the EPOC phenomenon in the ethanol steam reforming reaction. For that purpose, a Pt-KβAl₂O₃ electrochemical catalyst has been prepared, characterized and tested under ethanol reforming reaction conditions. The obtained results show potential for the application of the EPOC phenomenon for the enhancement of catalytic activity and selectivity in hydrogen production from ethanol reforming as well as for the in-situ catalyst regeneration from carbon deposition. The use of EPOC, coupled with different in-situ and ex-situ characterization techniques, allows to study the mechanism of ethanol reforming reaction leading to valuable conclusions for the scientific catalysis community.

2. Experimental

2.1. Electrochemical catalyst preparation

An electrically continuous Pt film (geometric area of 2.01 cm²) was deposited on a 20-mm-diameter, 1-mm-thick K-βAl₂O₃ (Ionotec) solid electrolyte disc using Au as counter and reference electrodes on the solid electrolyte cell. Firstly, Au counter and reference electrodes were deposited on one side of the K-βAl₂O₃ disc by applying thin coatings of gold paste (Gwent Electronic Materials), followed by calcination at 800 °C for 2 h (heating ramp of 5 °C/min). Au was chosen due to its catalytically inactive properties for the ethanol reforming reaction as verified by blank experiments. Then, the active Pt catalyst / working electrode (W) was deposited on the other side of the solid electrolyte, as described in detail elsewhere [38], by the impregnation of a H₂PtCl₆ solution, followed by calcination at 800 °C for 2 h (heating ramp of 5 °C/min). The final Pt metal loading on the solid electrolyte cell was 1.05 mg_{Pt} cm⁻². Before the catalytic activity measurements, a temperature programmed reduction treatment was performed under a 5% H₂ stream (Ar balance, total flow = 100 mL/min (Standard Ambient Temperature and Pressure, SATP)) from room temperature to 450 °C (ramp of 5 °C/min).

2.2. Catalytic activity measurements

The catalytic activity measurements were carried out in an experimental setup used in previous studies [38], using a single chamber solid electrolyte cell reactor configuration [39]. The reaction gases (Praxair, Inc) were certified standards (99.999% purity) of Ar (99.999% purity, carrier gas), H₂ (99.999% purity, reducing agent) and O₂ (99.999% purity, oxidizing agent). Ethanol (Panreac, 99.8% purity) and water (distilled and deionized) were fed by sparging Ar through thermostated saturators and a set of mass flowmeters (Bronkhorst EL-FLOW) controlled the gas flow rates.

The catalytic experiments were carried out at atmospheric pressure and a temperature ranging from 400 to 500 °C, with an overall gas flow rate of 100 mL/min (SATP) and a composition of C₂H₅OH / H₂O = 3%/9% (Ar balance). Reactant and product gases were online analyzed by using a double channel gas chromatograph (Bruker 450-GC) equipped with Hayesep and Q-Molsieve 13X consecutive columns and a CP-Wax 52 CB column, along with thermal conductivity (TCD) and flame ionization (FID) detectors, respectively. The detected products were: H₂, CO₂ and acetaldehyde (C₂H₄O).

The three electrodes were connected to an Autolab PGSTAT320-N potentiostat-galvanostat (Metrohm Autolab) using gold wires (Alfa Aesar, 99.95% purity). The EPOC experiments were carried out by applying different electrical currents measured between the working and counter electrodes; and potentials, measured between the working and reference electrodes (V_{WR}), according to the procedure generally used in conventional three-electrode electrochemical cells [28].

2.3. Electrochemical catalyst characterization

Different techniques were used for the in-situ and ex-situ characterization of the electrochemical catalyst to support the obtained catalytic results.

In the first place, temperature programmed oxidation (TPO) experiments were in-situ performed using a 2% O₂ stream (Ar balance, total flow = 100 mL/min (SATP)) and temperature range from 150 to 550 °C (heating ramp 2 °C/min) in order to evaluate the presence of carbon formed on the catalyst surface during catalytic experiments.

Raman spectra of the Pt catalyst film after EPOC experiments were also obtained from the Pt catalyst surface with a SENTERRA spectrometer with a grating of 600 lines per mm and a laser wavelength of 532 nm at a very low laser power level (< 1 mW), to avoid any heating effect. The Pt film after catalysis testing was also studied with Scanning Electron Microscopy (SEM) (Phenom ProX) with a field emission gun with a resolution of 15 kV and a magnification of 2000 × . Elemental analysis was carried out with Energy-dispersive X-ray spectroscopy (EDX) (Phenom ProX).

3. Results and discussion

3.1. Electrochemical promotion of the Pt catalyst

The phenomenon of Electrochemical Promotion was firstly investigated by a combined galvanostatic-potentiostatic transient at 500 °C. Fig. 1 shows the response of the hydrogen production rate and the catalyst potential (V_{WR}) vs. time during the application of different potentiostatic and galvanostatic transients: a positive potential (V_{WR} = + 2 V) for 62 min, a negative current (I = -10 μA, current density: j = -4.97 μA·cm⁻²) for 88 min, open circuit potential (OCV) for 62 min and a final positive potential (V_{WR} = + 2 V) for 25 min.

As typically found with electrochemical catalysts based on alkaline ionic conductors [40], such as K-βAl₂O₃ (present case), positive alkali ions may have thermally migrated from the solid electrolyte to the catalyst surface during the catalyst preparation and reduction step [41]. Hence, at the beginning and at the end of each experiment, a positive potential (V_{WR} = + 2 V), higher than the open circuit potential, is

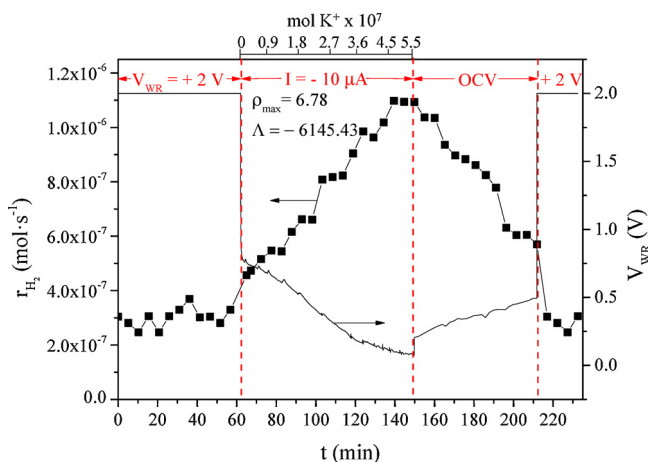


Fig. 1. Variations of H_2 production rates vs. time upon different potentiostatic and galvanostatic transitions. Ethanol steam reforming conditions: $\text{C}_2\text{H}_5\text{OH}/\text{H}_2\text{O} = 3\%/\text{9}\%$, Ar balance. $T = 500^\circ\text{C}$.

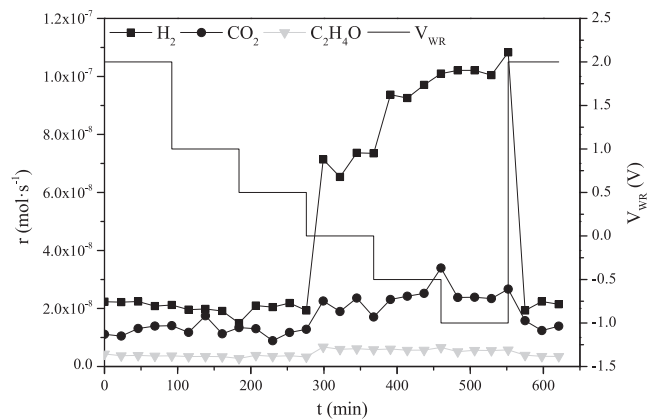


Fig. 2. Variations of H_2 , CO_2 and $\text{C}_2\text{H}_4\text{O}$ production rates vs. time upon different potentiostatic transitions. Ethanol steam reforming conditions: $\text{C}_2\text{H}_5\text{OH}/\text{H}_2\text{O} = 3\%/\text{9}\%$, Ar balance. $T = 450^\circ\text{C}$.

applied in order to remove from the catalyst the possible migrated ions leading to a clean Pt catalyst film, free of promoter, established as a reference state (unpromoted).

During the negative galvanostatic step, potassium ions were electrochemically transferred to the catalyst surface at a rate $I/nF = 1.04 \cdot 10^{-10} \text{ mol}_{\text{K}^+} \cdot \text{s}^{-1}$ according to the Faraday equation. It can be observed that the increase on the potassium supply enhanced the hydrogen production rates leading to an electrophilic behaviour according to the rules of electrochemical promotion of catalysis [42], i.e. its rate increases with decreasing catalyst potential and hence catalyst work function. This enhancement can be attributed to an increase of intermediate chemisorbed species (ethoxy molecules) and its further dehydrogenation as will be explained below. At the same time, a decrease in the potential measured between the working and reference electrodes (V_{WR}) was observed during the application of the negative current following the same trend than previous studies with alkali solid electrolytes [43,44]. Then it is clear that the back-spillover of potassium ions onto the catalyst film under the applied negative current led to a strong activation of the catalyst that can be quantified by the following electrochemical promotional parameters: ρ (reaction rate enhancement ratio) and Λ (Faradaic efficiency), which are defined according to the following equations [42]:

$$\rho = \frac{r}{r_0} \quad (2)$$

$$\Lambda = \frac{r - r_0}{I/nF} \quad (3)$$

where r and r_0 denote the promoted ($V_{\text{WR}} < +2 \text{ V}$) and unpromoted ($V_{\text{WR}} = +2 \text{ V}$) catalytic reaction rates, respectively; I the applied current (A), n is the potassium ion charge (+1, in this case), and F is the Faradaic constant (96485 C).

The values of these parameters shown on Fig. 1, clearly demonstrate the strong promotional effect induced during the negative polarization step, which allows to increase the hydrogen production rate in more than 3 times vs. the unpromoted catalyst surface. Hence, the high value of Faradaic efficiency demonstrates the strong promotional effect of K^+ ions in the catalytic reaction. Similar electro-promotional values have been reported in previous studies of EPOC in hydrogen production reactions with alkaline solid electrolytes. For instance, the reaction enhancement ratio (ρ) values of 2.5 for the partial oxidation of methanol and 3.4 for the reaction of steam reforming of methanol have been reported in a previous work [45].

On the other hand, it is also interesting to notice that once the current application was interrupted (open circuit conditions, at $t = 150 \text{ min}$), a decrease in hydrogen production rates occurred. Under these conditions, potassium ions were partially removed from the catalyst surface (thermal back-diffusion, sublimation...) [31,36], decreasing the hydrogen production rate. The final application of 2 V at $t = 212 \text{ min}$ forced the fast migration of K^+ promoters back to the solid electrolyte, leading to a strong decrease in the hydrogen production reaction until the unpromoted catalytic activity was again attained, achieving a complete reversible EPOC effect. This observation is in very good agreement with a recent study which has shown the immediate disappearance of the $\text{K}2\text{p}$ signal from a Ni catalyst film supported on $\text{K}-\beta''\text{Al}_2\text{O}_3$ under the application of 2 V studied by in-situ XPS measurements [46]. This fact points out the fully reversible character of the observed promotional effect as well as the stability of the catalyst film during the different polarization steps, i.e., the same catalytic activity at the beginning and at the end of the experiment was achieved under application of 2 V.

The variation of the different products reaction rates: H_2 , CO_2 , $\text{C}_2\text{H}_4\text{O}$ vs. time was investigated at different potentiostatic transients at 450°C , as shown in Fig. 2. In this case, different potentials were applied starting from the unpromoted state ($V_{\text{WR}} = +2 \text{ V}$) and applying lower electrical potential values for 115 min of duration each one. In this experiment, unlike the previous one, a steady state catalytic rate value was obtained after few minutes at each potential, since a fixed coverage of promoter is attained after few minutes at potentiostatic polarization [46].

It can be observed that a decrease in the applied potential below 0 V led to an increase in the different obtained product rates. In good agreement with the previous experiment, the electrochemical supply of K^+ ions at potentials lower than 0.5 V strongly activated the ethanol reforming activity on the Pt catalyst.

Attending to the obtained product rates, it is noticeable that the maximum hydrogen production rate was increased up to 5 times under application of -1 V vs. the unpromoted rate (2 V). It is interesting to note that this increase was more pronounced than the corresponding increase of the carbonaceous product rates (CO_2 and $\text{C}_2\text{H}_4\text{O}$). In fact, the ratio between the hydrogen production and the carbonaceous products rate ($\frac{r_{\text{H}_2}}{r_{\text{CO}_2} + r_{\text{C}_2\text{H}_4\text{O}}}$) in the unpromoted state (2 V) was 1.56, while at electro-promoted state (-1 V) this ratio was 3.53. At this point it should be noticed that the formation of new products were not detected by the GC analysis. This important difference indicates that some carbonaceous products may remain adsorbed on the catalyst surface during the negative polarization step. This kind of carbonaceous products have already been identified in previous works of catalytic steam reforming of ethanol in conventional Pt catalyst [47]. Hence, one could expect that a higher duration of the negative polarization steps may probably lead to a catalyst deactivation as will be shown later.

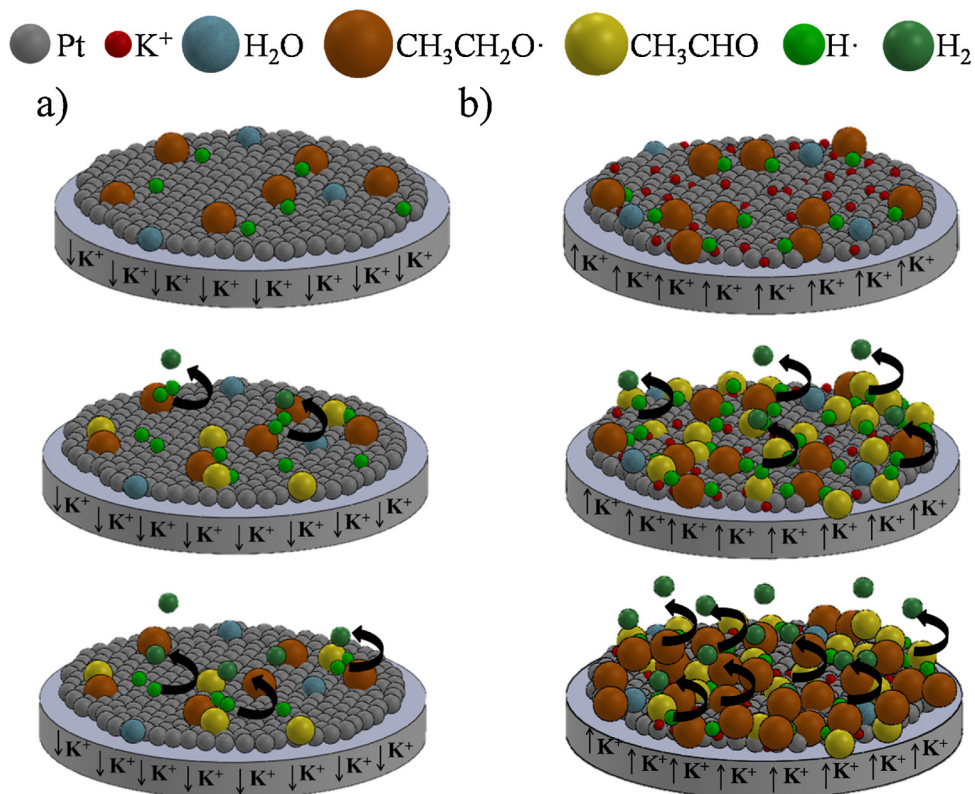


Fig. 3. Mechanism reaction scheme on the Pt catalyst surface: (a) unpromoted state (2 V), (b) promoted state (-1 V).

According to previous studies, during the ethanol steam reforming reaction, there are several reaction pathways that could take place depending on the catalysts used and their characteristics (metal dispersion, thermal stability, metal-support interaction, particle size) as well as operational parameters such as reaction temperature [48,49]. The ethanol adsorption on the catalyst surface (Reaction (4)) is the first step in the reaction mechanism of ethanol reforming [48,50]. Once ethanol is adsorbed, the dehydrogenation is produced by two consecutive reactions: ethanol is firstly dehydrogenated to an intermediate ethoxy molecule (Reaction (5)) and then into acetaldehyde (Reaction (6)) [25]. Hydrogen can be produced via recombination of H adsorbed atoms (Reaction (7)) and via acetaldehyde steam reforming reaction (Reaction (8)). Finally, the water gas shift reaction (Reaction (9)) occurred leading to the further production of H₂ and CO₂.



According to the obtained results one can suggest that under unpromoted conditions (2 V), the ethanol dehydrogenation reactions (Reactions (5) and (6)) which initiated the process were the rate-determining step [51]. Under these conditions, the hydrogen production was limited by the presence of a low coverage of intermediate ethoxy and acetaldehyde adsorbed molecules, leading to a low hydrogen production rate and almost a stoichiometric $\frac{r_{\text{H}_2}}{r_{\text{CO}_2} + r_{\text{C}_2\text{H}_4\text{O}}}$ value [52]. On the other hand, the presence of K⁺ during the negative polarization steps, at the promoted conditions, activated the ethanol dehydrogenation reactions (Reactions (5) and (6)). The observed electrophilic behavior

can be explained considering the strengthening of the chemisorptive bond of electron acceptor molecules, i.e., intermediate ethoxy molecules, with decreasing catalyst work function. It increases the stability of these intermediates and favors their formation. A similar electrophilic effect has been reported for the case of methanol decomposition considering the electron acceptor character of intermediate methoxy molecules formed in these previous cases [30,53]. Under these conditions, the hydrogen production rate may have probably increased via Reaction (7) while very likely a large amount of ethoxy species and acetaldehyde molecules remained adsorbed on the Pt active sites, which explains the increase in the $\frac{r_{\text{H}_2}}{r_{\text{CO}_2} + r_{\text{C}_2\text{H}_4\text{O}}}$ ratio during the negative polarization step.

This Electrochemical Promotion mechanism is schematized on Fig. 3 and further supported by the influence of the partial pressure of water ($p_{\text{H}_2\text{O}}$) (Fig. 4a) and ethanol ($p_{\text{C}_2\text{H}_5\text{OH}}$) (Fig. 4b) on the steady-state H₂ production rate at 450 °C, upon the imposition of two different potentials: +2 V (unpromoted state) and -1 V (promoted state).

It is clear that under all the explored reaction conditions, the activity of the catalyst for hydrogen production was enhanced under the negative polarization due to the previous mentioned activation of dehydrogenation reaction steps (Reactions (5) and (6)). On the other hand, it can be observed that under absence of promoter the hydrogen production remained nearly constant vs. the partial pressure of water, showing a zero apparent reaction order with respect to water, in good agreement with previous studies [54]. Under these conditions, as already mentioned, the process is limited by the initial dehydrogenation reaction steps and, hence, by the low coverage of ethoxy and acetaldehyde adsorbed molecules, leading to an almost negligible effect of water coverage. However, under promoted conditions (-1 V), a positive order of water molecules is initially observed due to the higher coverage of adsorbed ethoxy and acetaldehyde adsorbed molecules under presence of potassium, which activated the hydrogen production via Reaction (8). At higher values of partial pressure of water ($p_{\text{H}_2\text{O}} > 0.08$ bar) Reaction (8) started to be limited by a high relative

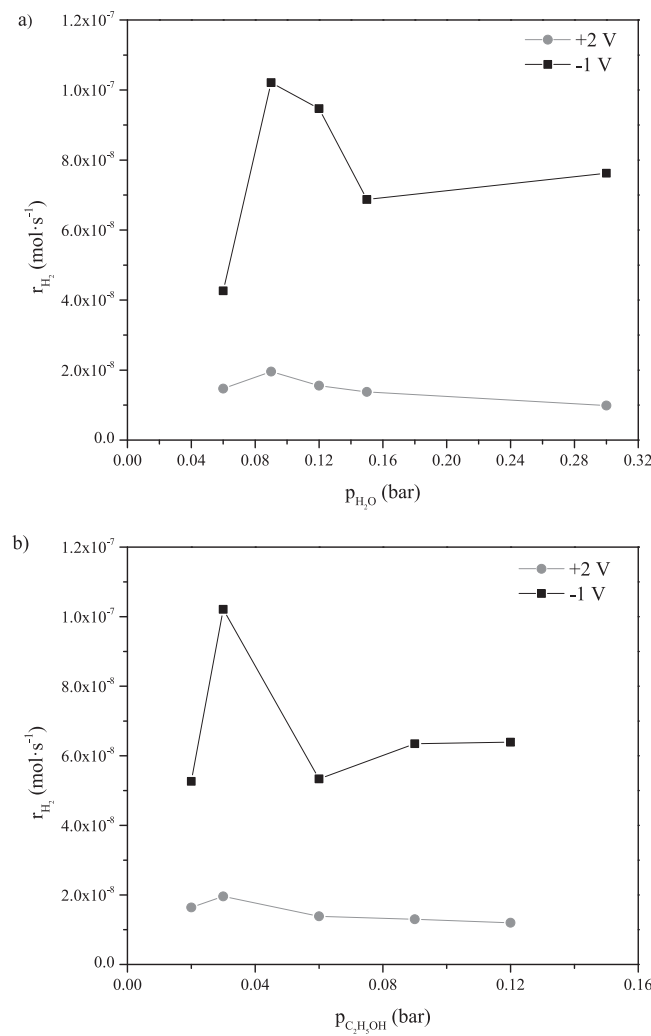


Fig. 4. Effect of the H₂O (a) and C₂H₅OH (b) partial pressures on the H₂ under unpromoted (+2 V) and promoted (-1 V) conditions. Ethanol steam reforming conditions: C₂H₅OH/H₂O = 3% / 9%. T = 450 °C.

coverage of water/acetaldehyde molecules, leading to a negative order of water molecules. This competitive adsorption between water and acetaldehyde justifies the presence of an optimal coverage at a partial pressure of 0.09 bar, typical of Langmuir-Hinshelwood mechanism where the two molecules are competitively adsorbed on neighboring sites [55].

The partial pressure of ethanol, under absence of promoter, barely affects the hydrogen production as happened in the case of the partial pressure of water. Under these conditions, the increase in the coverage of ethanol adsorbed molecules is not enough to initiate the process since the dehydrogenation reactions rates were limited under absence of promoter. It demonstrates again that the process is limited by Reactions (5) and (6) and not by the initial adsorption of ethanol (Reaction (4)). Under promoted conditions (-1 V), an increase in the partial pressure of ethanol led to an initial positive effect on the hydrogen production. As already commented, the presence of promoter activated the stabilization of ethoxy intermediate species which initiated the process, thus leading to hydrogen production via Reaction (8). Under these conditions, acetaldehyde steam reforming reaction became the rate-determining step. At higher values of partial pressure of ethanol (p_{C₂H₅OH} > 0.03 bar) the reaction mechanism was limited by the high coverage of ethoxy and acetaldehyde molecules which remained adsorbed on the catalyst surface. Therefore, the lower relative coverage of water/acetaldehyde led to a negative effect on hydrogen

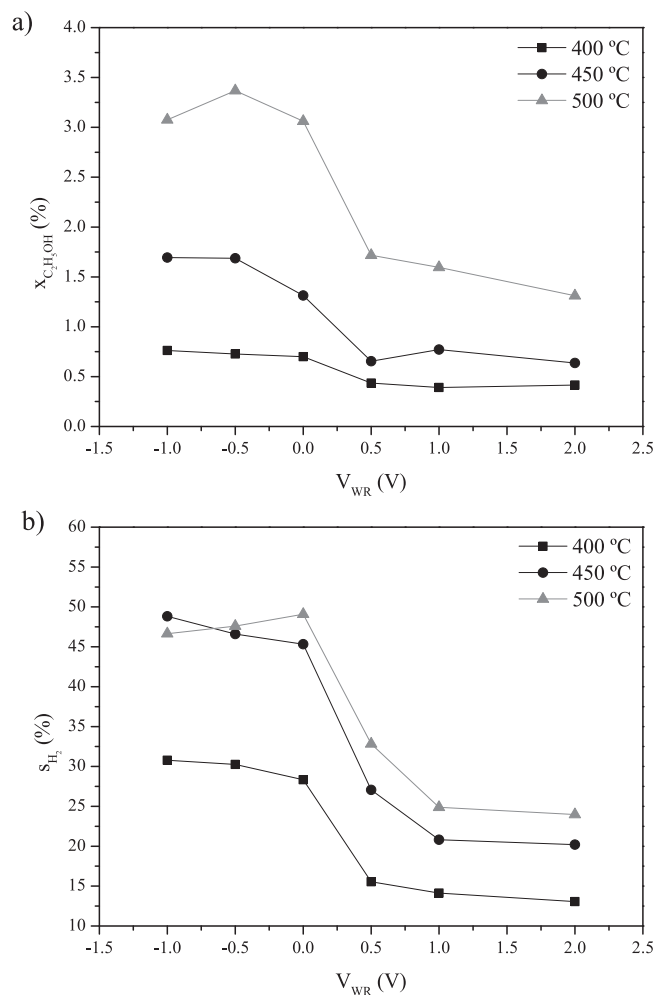


Fig. 5. Steady state C₂H₅OH conversion (a) and H₂ selectivity (b) vs. applied potential (V_{WR}) at different reaction temperatures. Ethanol steam reforming conditions: C₂H₅OH/H₂O = 3% / 9%.

production.

The steady state variation of the ethanol conversion and catalyst selectivity vs. the applied potential were evaluated at different reaction temperatures, as shown in Fig. 5. In these experiments, different potentiostatic transients were applied (from +2 V to -1 V, returning to +2 V), for 115 min each one until a steady state catalytic rate value was achieved. The ethanol conversion and the hydrogen selectivity were calculated as follows:

$$x_{C_2H_5OH}(\%) = \frac{(F_{C_2H_5OH,in} - F_{C_2H_5OH,out})}{F_{C_2H_5OH,in}} \cdot 100 \quad (10)$$

$$s_{H_2}(\%) = \frac{F_{H_2,out}}{6 \cdot (F_{C_2H_5OH,in} - F_{C_2H_5OH,out})} \cdot 100 \quad (11)$$

where F_{i,in} and F_{i,out} are the molar flow rate of the i species at the inlet and outlet of the reactor, respectively.

Firstly, it can be observed that under all the explored reaction temperatures, the catalytic activity of the system was enhanced decreasing the applied potential, i.e., an electrophilic EPOC behavior was obtained in the whole temperature range [42]. On the other hand, the ethanol conversion increased with the reaction temperature due to the increase in the reaction kinetics. It can also be observed that the electrochemical activation effect was higher at higher reaction temperatures. This behaviour can be easily explained considering the exponential effect of reaction temperature on the dehydrogenation kinetics (Reactions (5) and (6)). On the other hand, it can be observed

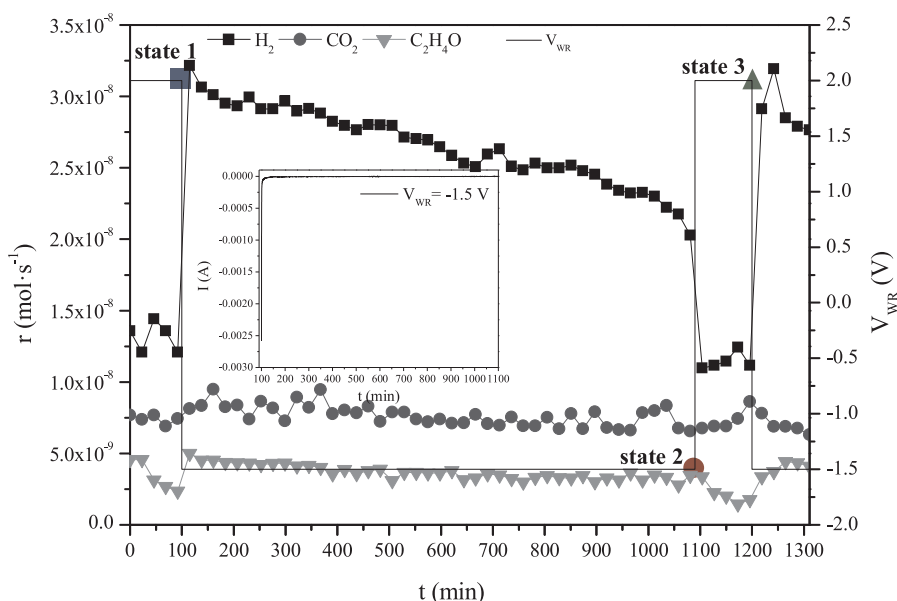


Fig. 6. H₂, CO₂ and C₂H₄O production rates variation vs. time for a long EPOC experiment during a mild-term. Ethanol steam reforming conditions: C₂H₅OH/H₂O = 3% / 9%. T = 400 °C.

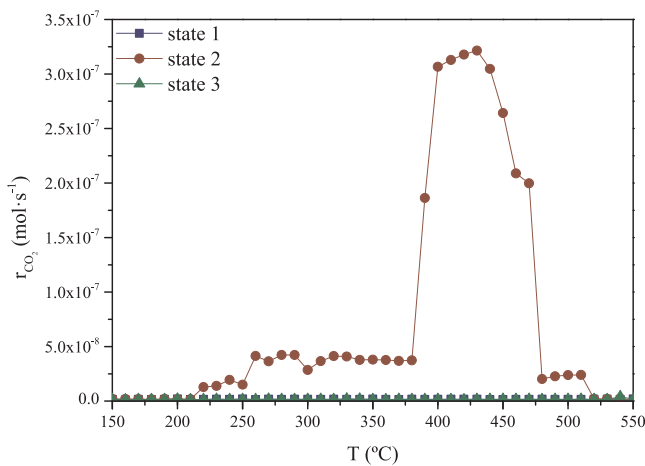


Fig. 7. CO₂ production rates vs. temperature in a temperature programmed oxidation at three different states (pointed out in Fig. 6.). O₂ = 2% (Ar balance), heating ramp 2 °C·min⁻¹.

that an optimal potential value of -0.5 V was achieved at 500 °C. The application of more negative potentials led to an excess of promoter coverage on the catalyst surface (the ionic conductivity of the electrolyte and hence the ion migration increased with the reaction temperature at fixed potentials). It may poison catalytic active sites as it has been already observed in previous studies of EPOC with alkaline conductors on methanol reforming reactions [36]. From these experiments, it is clear that EPOC allows to optimize the amount of potassium coverage on the catalyst surface at varying reaction conditions, which is not possible with conventional catalytic promoters [52,56]. On the other hand, it can be observed that ethanol conversion was kept below 4% at all the explored reaction temperatures. It is due to the low geometric area of the catalyst film (2.01 cm^2), a high reactant bypass to the catalyst surface on the used single chamber reactor cell and to the low catalytically active surface area of the catalyst film [38]. This kind of reactor configuration is suitable for lab scale studies. However, other reactor designs, e.g., the monolithic electro-promoted reactor (MEPR), should be used for practical applications, in order to get higher catalyst-surface area and higher catalytic conversions values [57]. Regarding the catalyst selectivity to hydrogen production, it is also interesting to

note the positive effect of the electrochemical promoter. As already explained, it is due to the increase in the kinetic of the dehydrogenation reactions (Reactions (5) and (6)), which allows to produce a higher relative amount of hydrogen vs. carbonaceous molecules. The possibility of modifying in situ the product selectivity of the catalyst is also one of the main interests of the EPOC phenomenon and it has been studied in a large number of catalytic reactions such as CO₂ hydrogenation [58], selective catalytic reduction of NO_x [38] or methanol partial oxidation [30].

3.2. Stability study and characterization of the Pt catalyst

In order to check the stability of the catalyst, Fig. 6 shows a mild term negative polarization step ($V_{WR} = -1.5$ V) which was applied for 15 h at 400 °C. The inset of the figure also depicts the variation of the current vs. time during the negative potentiostatic polarization step.

As already observed in previous studies [46], the migration of the potassium ions occurred during the first seconds of the potentiostatic polarization, as can be observed from the trend of the current vs. time, which leads to faradaic ions migration rate (I/nF). As already observed from previous experiments, the electrochemical supply of potassium enhanced the hydrogen production rate. However, a continuous decrease in the catalytic activity along the time can be observed during the mild term polarization step. As already mentioned, it could be attributed to the continuous formation and adsorption of intermediate carbonaceous species, which block the Pt active sites, induced by the fixed coverage of potassium ions achieved at the beginning of the polarization [59]. As already mentioned, the presence of the electrochemical promoter activated dehydrogenation reactions (Reactions (5) and (6)) which initiated the ethanol reforming mechanism, leading to the formation and adsorption of a growing amount of carbonaceous molecules that cause the observed deactivation. However, it can also be observed that the application of an electric potential of 2 V allowed to regenerate the catalyst from such carbonaceous species, i.e., the electro-promoted catalytic activity was fully recovered in the second polarization step at -1.5 V (at $t = 1200$ min), leading to a fully reversible effect. The application of +2 V allowed to achieve the initial coverage of reactant species (un-promoted catalyst state) in agreement with the experiment of Fig. 1, i.e., the enhancement of intermediate ethoxy molecules chemisorption and adsorption stopped, achieving the initial catalytic activity at the beginning of the experiment ($t = 0$ –100 min). It

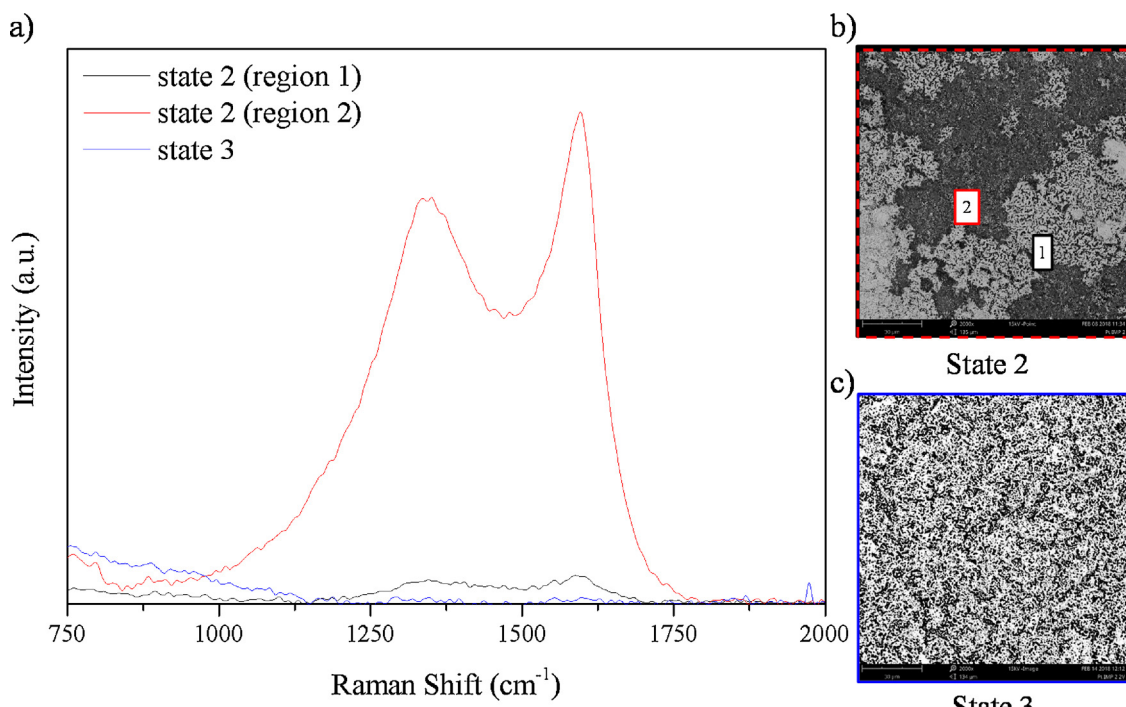


Fig. 8. Raman spectra (a) of Pt catalysts after different applied potentials at Fig. 6 reaction conditions and microscopy images after different states: state 3 (b) and state 2.

allows to recover a catalyst surface free of adsorbed carbonaceous molecules that can be again electrochemically activated in a second negative polarization step at $t = 1200$ min.

Similar activation/regeneration cycles induced by the applied polarization have already been demonstrated on previous studies on reforming and partial oxidation of methane [31]. These results can be supported by in-situ temperature programmed oxidation experiments (TPO) performed just after each polarization step denoted as following: *state 1* after the initial polarization at 2 V at $t = 100$ min, *state 2* after the polarization at -1.5 V at $t = 1090$ min and *state 3* after the second polarization at 2 V at $t = 1200$ min. Fig. 7 shows the CO_2 production rate obtained during the temperature-programmed oxidation experiments performed between 150 and 550 °C under 2% O_2 Ar balance, stream. From the obtained results, it can be observed that under *state 1* and *state 3*, the catalyst surface was free from carbonaceous products due to the absence of CO_2 during the TPO experiment. It implies that the application of 2 V allows to obtain a catalyst surface free of intermediate carbonaceous molecules. In contrast, after 15 h under application of -1.5 V (*state 2*), the temperature-programmed oxidation showed a large amount of CO_2 coming from the presence of carbonaceous species deposited on catalyst surface. The formation of this large amount of carbon molecules is, therefore, induced by the negative polarization, i.e., the presence of K^+ activate dehydrogenation reactions (Reactions (5) and (6)) via strengthening of ethoxy intermediate molecules chemisorption and stabilization. These conclusions were further confirmed by two ex-situ characterization techniques: Raman Spectroscopy (Fig. 8) and SEM-EDX (Fig. 9) analysis performed on the Pt catalyst film under *state 2* and *3*.

Raman spectroscopy is considered a very interesting tool in the study of formation of carbon species during catalytic experiments [60]. Three different analysis can be observed in Fig. 8: one of them shows the spectrum of the catalyst surface under *state 3*, and the other two show the spectra of the catalyst surface under *state 2*. On this latter case (*state 2*), two regions were clearly observed: a first region corresponding to an apparently clean electrode zone (*region 1*) and the second one in a darker zone (*region 2*), where carbonaceous species deposition was visible at first sight. While the spectra corresponding to

state 3 and *region 1* of *state 2* did not show any peak, the spectra obtained on *region 2* of *state 2* showed two peaks, one of them at 1348 cm^{-1} (D band) and the other at 1595 cm^{-1} (G band), identified as the disordered graphitic lattice and ideal graphitic lattice, respectively. This kind of adsorbed carbonaceous products have been identified as the main cause of the deactivation of reforming catalysts, and their structure is determined by the hydrogen/hydrocarbon ratio in the feed, and the nature of the metallic phase. The spectrum corresponding to the *region 2* of *state 2* resemble a carbonaceous structure closely of pre-graphitic carbon observed in Pt catalysts [61]. The D band has been often ascribed to the vibrations of CH_3 group, vibration of olefin and aromatic species and the G band to the stretching vibrations of highly ordered sp^2 graphitic [62], although it could be also attributed to olephinic chains in carbonaceous deposit [63].

Fig. 9 shows the SEM micrographs along with its corresponding EDX analysis of the Pt film under *state 3* (Fig. 9a) and *state 2* (Fig. 9b) of the Pt catalyst film.

The first micrograph (Fig. 9a) shows a homogeneous and porous clean Pt surface. However, two different regions are observed in the second micrograph corresponding to *state 2*. According to the EDX analysis, the lighter region corresponds to Pt, while the darker region corresponds to a carbonaceous surface compound, probably a combination of adsorbed carbonaceous species, as already observed in previous studies [59]. All these results confirm the electrochemical promotion mechanism proposed for the Ethanol Steam Reforming Reaction and the possibility of using this phenomenon for the in-situ activation of catalytic activity and selectivity of hydrogen production, as well as the possibility of catalyst regeneration from carbon deposition.

4. Conclusions

The following conclusions could be drawn from this study:

- The obtained results showed the interest of electrochemistry to improve the activity and selectivity of a Pt catalyst in the H_2 production from ethanol via steam reforming (ESR).
- The electrochemical supply of potassium ions to a Pt catalyst film

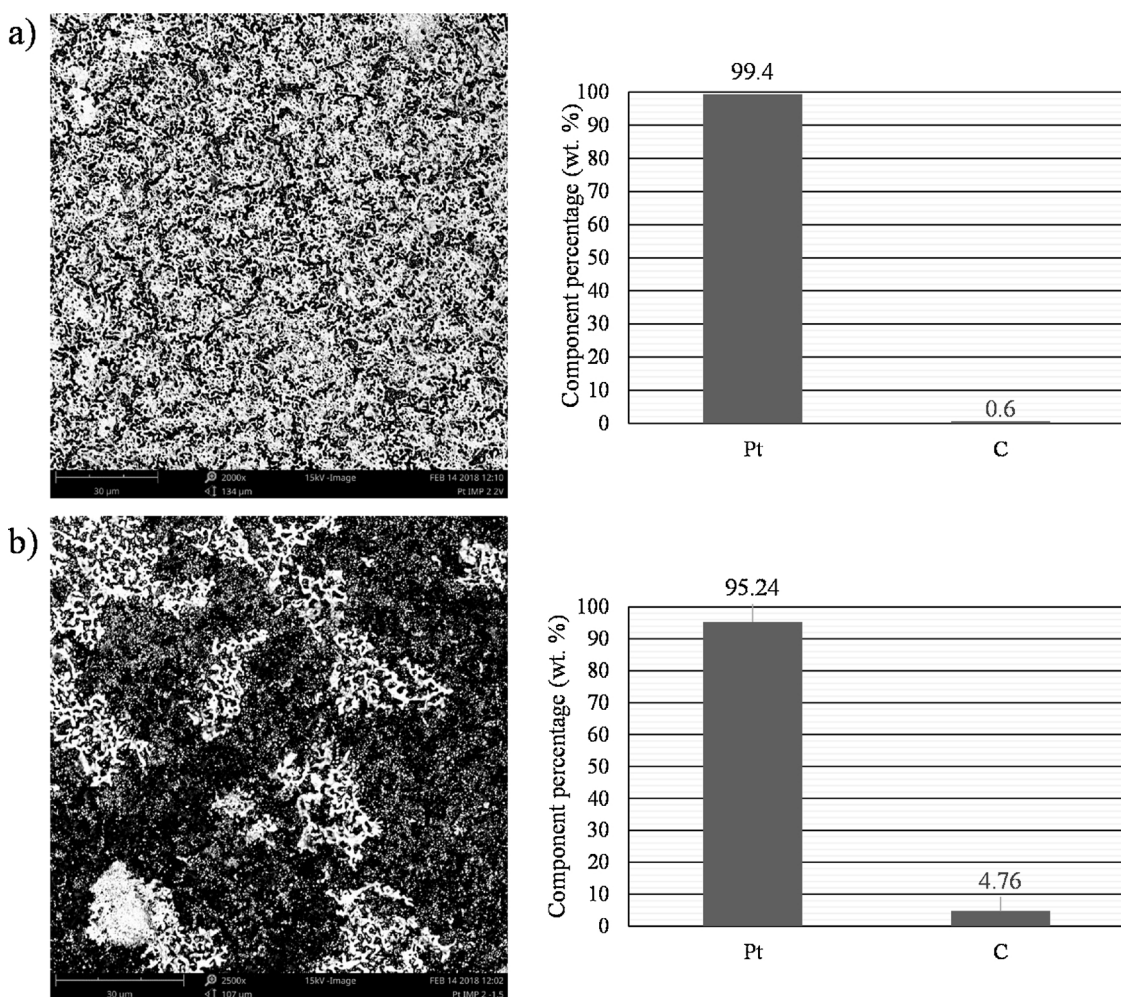


Fig. 9. Top surface SEM micrographs of the Pt catalysts after EPOC experiments ($\text{C}_2\text{H}_5\text{OH}/\text{H}_2\text{O} = 3\%/9\%$, 400°C) at state 3 (a) and state 2 (b), along with the corresponding EDX analysis of the shown region.

allows to strongly enhance the hydrogen production rate. This promotional effect has been attributed to the enhancement of the kinetic of ethanol dehydrogenation reaction, due to the strengthening of the chemisorptive bond of intermediate ethoxy molecules. It increases the stability of these intermediates and favors their formation, which initiates the ethanol reforming process.

- Under presence of the electrochemical promoter, intermediate carbonaceous species remained adsorbed on the catalyst surface, leading to a catalyst deactivation. However, these species were completely removed by applying a positive potential of 2 V as supported by different in-situ and ex-situ characterization techniques.
- The EPOC phenomenon serves as an additional tool to study the mechanism of catalytic reactions as well as to tune the adsorption of reactants molecules on the catalyst surface. This latter may have strong importance in hydrogen production technology for the in-situ controlling hydrogen production rates in non-stationary process (e.g., in-situ hydrogen production in mobile applications).

Funding sources

This work was supported by Spanish Ministry of Economy and Competitiveness [project CTQ2016-75491-R].

Acknowledgment

The authors gratefully acknowledge Spanish Ministry of Economy

and Competitiveness for the financial support of this work.

References

- [1] A. Campen, K. Mondal, T. Wiltowski, Separation of hydrogen from syngas using a regenerative system, *Int. J. Hydrogen Energy* 33 (2008) 332–339, <https://doi.org/10.1016/j.ijhydene.2007.07.016>.
- [2] E. Guicciardi, V. Chiodo, S. Freni, S. Cavallaro, A. Galvagno, J.C.J. Bart, Ethanol and dimethyl ether steam reforming on Rh/ Al_2O_3 catalysts for high-temperature fuel-cell feeds, *React. Kinet. Mech. Catal.* 104 (2011) 75–87, <https://doi.org/10.1007/s11144-011-0335-y>.
- [3] F. Liu, L. Zhao, H. Wang, X. Bai, Y. Liu, Study on the preparation of Ni-La-Ce oxide catalyst for steam reforming of ethanol, *Int. J. Hydrogen Energy* 39 (2014) 10454–10466, <https://doi.org/10.1016/j.ijhydene.2014.05.036>.
- [4] T. Mondal, K.K. Pant, A.K. Dalai, Oxidative and non-oxidative steam reforming of crude bio-ethanol for hydrogen production over Rh promoted Ni/ $\text{CeO}_2\text{-ZrO}_2$ catalyst, *Appl. Catal. A Gen.* 499 (2015) 19–31, <https://doi.org/10.1016/j.apcata.2015.04.004>.
- [5] C. Pirez, W. Fang, M. Capron, S. Paul, H. Jobic, F. Dumeignil, L. Jalowiecki-Duhamel, Steam reforming, partial oxidation and oxidative steam reforming for hydrogen production from ethanol over cerium nickel based oxyhydride catalyst, *Appl. Catal. A Gen.* 518 (2016) 78–86, <https://doi.org/10.1016/j.apcata.2015.10.035>.
- [6] A.G. da Silva, P.A. Robles-Dutnephner, A. Dias, H.V. Fajardo, A.S. Lovón, J.J. Lovón-Quintana, G.P. Valençoa, Gold, palladium and gold–palladium supported on silica catalysts prepared by sol–gel method: synthesis, characterization and catalytic behavior in the ethanol steam reforming, *J. Sol-Gel Sci. Technol.* 67 (2013) 273–281, <https://doi.org/10.1007/s10971-013-3076-8>.
- [7] D. Ghita, D.S. Ezeanu, D. Cursaru, P. Rosca, Hydrogen production by steam reforming of bioethanol over Pt based catalysts, *Rev. Chim.* 67 (2016) 145–149.
- [8] M. Bilal, S.D. Jackson, Ethanol steam reforming over Pt/ Al_2O_3 and Rh/ Al_2O_3 catalysts: the effect of impurities on selectivity and catalyst deactivation, *Appl. Catal. A Gen.* 529 (2017) 98–107, <https://doi.org/10.1039/C2CY20703F>.

- [9] K. Mudiyanselage, I. Al-Shankiti, A. Foulis, J. Llorca, H. Idriss, Reactions of ethanol over CeO₂ and Ru/CeO₂ catalysts, *Appl. Catal. B* 197 (2016) 198–205, <https://doi.org/10.1016/j.apcatb.2016.03.065>.
- [10] Z. Ferencz, E. Varga, R. Puskás, Z. Kónya, K. Baán, A. Oszkó, A. Erdőhelyi, Reforming of ethanol on Co/Al₂O₃ catalysts reduced at different temperatures, *J. Catal.* 358 (2018) 118–130, <https://doi.org/10.1016/j.jcat.2017.12.003>.
- [11] S. Turczyński, M. Greluk, G. Słowik, W. Gac, S. Zafeiratos, A. Machocki, Surface state and catalytic performance of ceria-supported cobalt catalysts in the steam reforming of ethanol, *ChemCatChem* 9 (2017) 782–797, <https://doi.org/10.1002/cctc.201601343>.
- [12] I. Deinega, L.Y. Dolgykh, L. Staraya, P. Strizhak, E. Moroz, V. Pakharukova, Catalytic properties of nanosized Cu/ZrO₂ systems in the steam reforming of bioethanol, *Theor. Exp. Chem.* 50 (2014) 46–52, <https://doi.org/10.1007/s11237-014-9347-9>.
- [13] A.A. Gonçalves, P.B. Faustino, J.M. Assaf, M. Jaroniec, One-pot synthesis of mesoporous Ni-Ti-Al ternary oxides: highly active and selective catalysts for steam reforming of ethanol, *ACS Appl. Mater. Interfaces* 9 (2017) 6079–6092, <https://doi.org/10.1021/acsm.6b15507>.
- [14] J.H. Song, S.J. Han, I.K. Song, Hydrogen production by steam reforming of ethanol over mesoporous Ni-Al₂O₃-ZrO₂ catalysts, *Catal. Surv. Asia* (2017) 1–16, <https://doi.org/10.1016/j.ijhydene.2013.09.114>.
- [15] A.E.P. de Lima, D.C. de Oliveira, In situ XANES study of cobalt in Co-Ce-Al catalyst applied to steam reforming of ethanol reaction, *Catal. Today* 283 (2017) 104–109, <https://doi.org/10.1016/j.cattod.2016.02.029>.
- [16] L.-C. Chen, S.D. Lin, The ethanol steam reforming over Cu-Ni/SiO₂ catalysts: effect of Cu/Ni ratio, *Appl. Catal. B* 106 (2011) 639–649, <https://doi.org/10.1016/j.apcatb.2011.06.028>.
- [17] M. Greluk, G. Słowik, M. Rotko, A. Machocki, Steam reforming and oxidative steam reforming of ethanol over PtKCo/CeO₂ catalyst, *Fuel* 183 (2016) 518–530, <https://doi.org/10.1016/j.fuel.2016.06.068>.
- [18] A.C. Furtado, C.G. Alonso, M.P. Cantão, N.R.C. Fernandes-Machado, Bimetallic catalysts performance during ethanol steam reforming: influence of support materials, *Int. J. Hydrogen Energy* 34 (2009) 7189–7196, <https://doi.org/10.1016/j.ijhydene.2009.06.060>.
- [19] J. Dobosz, M. Małecka, M. Zawadzki, Hydrogen generation via ethanol steam reforming over Co/HAp catalysts, *J. Energy Inst.* 91 (3) (2017), <https://doi.org/10.1016/j.joei.2017.02.001>.
- [20] K. Wang, B. Dou, B. Jiang, Y. Song, C. Zhang, Q. Zhang, H. Chen, Y. Xu, Renewable hydrogen production from chemical looping steam reforming of ethanol using xCeNi/SBA-15 oxygen carriers in a fixed-bed reactor, *Int. J. Hydrogen Energy* 41 (2016) 12899–12909, <https://doi.org/10.1016/j.ijhydene.2016.05.100>.
- [21] K.M. Kim, B.S. Kwak, Y. Im, N.-K. Park, T.J. Lee, S.T. Lee, M. Kang, Effective hydrogen production from ethanol steam reforming using CoMg co-doped SiO₂@Co_{1-x}Mg_xO catalyst, *J. Ind. Eng. Chem.* 51 (2017) 140–152, <https://doi.org/10.1016/j.jiec.2017.02.025>.
- [22] J. Da Costa-Serra, A. Chica, Bioethanol steam reforming on Co/ITQ-18 catalyst: effect of the crystalline structure of the delaminated zeolite ITQ-18, *Int. J. Hydrogen Energy* 36 (2011) 3862–3869, <https://doi.org/10.1016/j.ijhydene.2010.12.094>.
- [23] M. Taghizadeh, F. Aghili, Recent advances in membrane reactors for hydrogen production by steam reforming of ethanol as a renewable resource, *Int. Rev. Chem. Eng.* (2018), <https://doi.org/10.1515/reve-2017-0083>.
- [24] M.-R. Li, G.-C. Wang, The mechanism of ethanol steam reforming on the Co₀ and Co₂₊ sites: a DFT study, *J. Catal.* 365 (2018) 391–404, <https://doi.org/10.1016/j.jcat.2018.07.002>.
- [25] L. Lang, S. Zhao, X. Yin, W. Yang, C. Wu, Catalytic activities of K-modified zeolite ZSM-5 supported rhodium catalysts in low-temperature steam reforming of bioethanol, *Int. J. Hydrogen Energy* 40 (2015) 9924–9934, <https://doi.org/10.1016/j.ijhydene.2015.06.016>.
- [26] M. Stoukides, C.G. Vayenas, The effect of electrochemical oxygen pumping on the rate and selectivity of ethylene oxidation on polycrystalline silver, *J. Catal.* 70 (1981) 137–146, [https://doi.org/10.1016/0021-9517\(81\)90323-7](https://doi.org/10.1016/0021-9517(81)90323-7).
- [27] I.V. Yentekakis, M. Konsolakis, R.M. Lambert, A. Palermo, M. Tikhov, Successful application of electrochemical promotion to the design of effective conventional catalyst formulations, *Solid State Ion.* 136–137 (2000) 783–790, [https://doi.org/10.1016/S0167-2738\(00\)00547-6](https://doi.org/10.1016/S0167-2738(00)00547-6).
- [28] D. Theleritis, S. Souentie, A. Siokou, A. Katsaounis, C.G. Vayenas, Hydrogenation of CO₂ over Ru/YSZ electropromoted catalysts, *ACS Catal.* 2 (2012) 770–780, <https://doi.org/10.1021/cs300072a>.
- [29] E. Baranova, A. Thursfield, S. Brosda, G. Foti, C. Cominellis, C. Vayenas, Electrochemical promotion of ethylene oxidation over Rh catalyst thin films sputtered on YSZ and TiO₂/YSZ supports, *J. Electrochem. Soc.* 152 (2005) E40–E49, <https://doi.org/10.1149/1.1839511>.
- [30] J. González-Cobos, D. López-Pedrajas, E. Ruiz-López, J. Valverde, A. de Lucas-Consuegra, Applications of the electrochemical promotion of catalysis in methanol conversion processes, *Top. Catal.* 58 (2015) 1290–1302, <https://doi.org/10.1007/s11244-015-0493-7>.
- [31] A. de Lucas-Consuegra, A. Caravaca, P.J. Martínez, J.L. Endrino, F. Dorado, J.L. Valverde, Development of a new electrochemical catalyst with an electrochemically assisted regeneration ability for H₂ production at low temperatures, *J. Catal.* 274 (2010) 251–258, <https://doi.org/10.1016/j.jcat.2010.07.007>.
- [32] S. Souentie, L. Lizarraga, A. Kambolis, M. Alves-Fortunato, J. Valverde, P. Vernoux, Electrochemical promotion of the water–gas shift reaction on Pt/YSZ, *J. Catal.* 283 (2011) 124–132, <https://doi.org/10.1016/j.jcat.2011.07.009>.
- [33] A. de Lucas-Consuegra, A. Caravaca, J. González-Cobos, J. Valverde, F. Dorado, Electrochemical activation of a non noble metal catalyst for the water–gas shift reaction, *Catal. Commun.* 15 (2011) 6–9, <https://doi.org/10.1016/j.catcom.2011.08.007>.
- [34] I. Yentekakis, Y. Jiang, S. Neophytides, S. Bebelis, C. Vayenas, Catalysis, electrocatalysis and electrochemical promotion of the steam reforming of methane over Ni film and Ni-YSZ cermet anodes, *Ionics* 1 (1995) 491–498, <https://doi.org/10.1007/BF02375296>.
- [35] A. Caravaca, A. de Lucas-Consuegra, C. Molina-Mora, J. Valverde, F. Dorado, Enhanced H₂ formation by electrochemical promotion in a single chamber steam electrolysis cell, *Appl. Catal. B* 106 (2011) 54–62, <https://doi.org/10.1016/j.apcatb.2011.05.004>.
- [36] J. González-Cobos, V.J. Rico, A.R. González-Elipe, J.L. Valverde, A. de Lucas-Consuegra, Electrochemical activation of an oblique angle deposited Cu catalyst film for H₂ production, *Catal. Sci. Technol.* 5 (2015) 2203–2214, <https://doi.org/10.1039/C4CY01524J>.
- [37] J. González-Cobos, J. Valverde, A. de Lucas-Consuegra, Electrochemical vs. chemical promotion in the H₂ production catalytic reactions, *Int. J. Hydrogen Energy* 42 (2017) 13712–13723, <https://doi.org/10.1016/j.ijhydene.2017.03.085>.
- [38] F. Dorado, A. de Lucas-Consuegra, P. Vernoux, J.L. Valverde, Electrochemical promotion of platinum impregnated catalyst for the selective catalytic reduction of NO by propane in presence of oxygen, *Appl. Catal. B* 73 (2007) 42–50, <https://doi.org/10.1016/j.apcatb.2006.12.001>.
- [39] I.V. Yentekakis, S. Bebelis, Study of the NEMCA effect in a single-pellet catalytic reactor. [Non-faradaic electrochemical modification of catalytic activity], *J. Catal.* (1992) 278–283, [https://doi.org/10.1016/0021-9517\(92\)90157-D](https://doi.org/10.1016/0021-9517(92)90157-D).
- [40] A. de Lucas-Consuegra, New trends of alkali promotion in heterogeneous catalysis: electrochemical promotion with alkaline ionic conductors, *Catal. Surv. Asia* 19 (2015) 25–37, <https://doi.org/10.1007/s10563-014-9179-6>.
- [41] I.V. Yentekakis, M. Konsolakis, R.M. Lambert, N. Macleod, L. Nalbantian, Extraordinarily effective promotion by sodium in emission control catalysis: no reduction by propane over Na-promoted Pt/γ-Al₂O₃, *Appl. Catal. B* 22 (1999) 123–133, [https://doi.org/10.1016/S0926-3373\(99\)00042-9](https://doi.org/10.1016/S0926-3373(99)00042-9).
- [42] C.G. Vayenas, *Electrochemical Activation of Catalysis: Promotion, Electrochemical Promotion, and Metal-Support Interactions*, Springer Science & Business Media, 2001.
- [43] J. González-Cobos, D. Horwat, J. Ghanbaja, J.L. Valverde, A. de Lucas-Consuegra, Electrochemical activation of Au nanoparticles for the selective partial oxidation of methanol, *J. Catal.* 317 (2014) 293–302, <https://doi.org/10.1016/j.jcat.2014.06.022>.
- [44] A. de Lucas-Consuegra, A. Princivalle, A. Caravaca, F. Dorado, C. Guizard, J.L. Valverde, P. Vernoux, Preferential CO oxidation in hydrogen-rich stream over an electrochemically promoted Pt catalyst, *Appl. Catal. B* 94 (2010) 281–287, <https://doi.org/10.1016/j.apcatb.2009.11.019>.
- [45] A. de Lucas-Consuegra, J. González-Cobos, V. Carcelén, C. Magén, J. Endrino, J. Valverde, Electrochemical promotion of Pt nanoparticles dispersed on a diamond-like carbon matrix: a novel electrocatalytic system for H₂ production, *J. Catal.* 307 (2013) 18–26, <https://doi.org/10.1016/j.jcat.2013.06.012>.
- [46] J.P. Espinós, V.J. Rico, J. González-Cobos, J.R. Sánchez-Valencia, V. Pérez-Dieste, C. Escudero, A. de Lucas-Consuegra, A.R. González-Elipe, In situ monitoring of the phenomenon of electrochemical promotion of catalysis, *J. Catal.* 358 (2018) 27–34, <https://doi.org/10.1016/j.jcat.2017.11.027>.
- [47] M. Kourtelesis, P. Panagiotopoulou, S. Ladas, X. Verykios, Influence of the support on the reaction network of ethanol steam reforming at low temperatures over pt catalysts, *Top. Catal.* 58 (2015) 1202–1217, <https://doi.org/10.1007/s11244-015-0485-7>.
- [48] J.L. Contreras, J. Salmones, J.A. Colín-Luna, L. Nuño, B. Quintana, I. Córdova, B. Zeifert, C. Tapia, G.A. Fuentes, Catalysts for H₂ production using the ethanol steam reforming (a review), *Int. J. Hydrogen Energy* 39 (2014) 18835–18853, <https://doi.org/10.1016/j.ijhydene.2014.08.072>.
- [49] R. González-Gil, C. Herrera, M.A. Larrubia, F. Mariño, M. Laborde, L.J. Alemany, Hydrogen production by ethanol steam reforming over multimetallic RhCeNi/Al₂O₃ structured catalyst. Pilot-scale study, *Int. J. Hydrogen Energy* 41 (2016) 16786–16796, <https://doi.org/10.1016/j.ijhydene.2016.06.234>.
- [50] M. Compagnoni, A. Tripodi, A. Di Michele, P. Sassi, M. Signoretto, I. Rossetti, Low temperature ethanol steam reforming for process intensification: new Ni/M_xO-ZrO₂ active and stable catalysts prepared by flame spray pyrolysis, *Int. J. Hydrogen Energy* 42 (2017) 28193–28213, <https://doi.org/10.1016/j.ijhydene.2017.09.123>.
- [51] T. Dong, Z. Wang, L. Yuan, Y. Torimoto, M. Sadakata, Q. Li, Hydrogen production by steam reforming of ethanol on potassium-doped 12CaO·7Al₂O₃ catalyst, *Catal. Lett.* 119 (2007) 29–39, <https://doi.org/10.1007/s10562-007-9148-z>.
- [52] M. Dömök, K. Baan, T. Kecskes, A. Erdőhelyi, Promoting mechanism of potassium in the reforming of ethanol on Pt/Al₂O₃ Catalyst, *Catal. Lett.* 126 (2008) 49–57, <https://doi.org/10.1007/s10562-008-9616-0>.
- [53] S. Neophytides, C.G. Vayenas, Non-faradaic electrochemical modification of catalytic activity: 2. The case of methanol dehydrogenation and decomposition on Ag, *J. Catal.* 118 (1989) 147–163, [https://doi.org/10.1016/0021-9517\(89\)90307-2](https://doi.org/10.1016/0021-9517(89)90307-2).
- [54] P. Giambelli, V. Palma, A. Ruggiero, Low temperature catalytic steam reforming of ethanol. 2. Preliminary kinetic investigation of Pt/CeO₂ catalysts, *Appl. Catal. B* 96 (2010) 190–197, <https://doi.org/10.1016/j.apcatb.2010.02.019>.
- [55] D.R. Sahoo, S. Vajpai, S. Patel, K.K. Pant, Kinetic modeling of steam reforming of ethanol for the production of hydrogen over Co/Al₂O₃ catalyst, *Chem. Eng. J.* 125 (2007) 139–147, <https://doi.org/10.1016/j.cej.2006.08.011>.
- [56] V. Palma, C. Ruocco, A. Ricca, Oxidative steam reforming of ethanol in a fluidized bed over CeO₂-SiO₂ supported catalysts: effect of catalytic formulation, *Renew. Energy* 125 (2018) 356–364, <https://doi.org/10.1016/j.renene.2018.02.118>.
- [57] D. Tsiplikides, S. Balomenou, Milestones and perspectives in electrochemically promoted catalysis, *Catal. Today* 146 (2009) 312–318, <https://doi.org/10.1016/j.cattod.2009.05.015>.

- [58] E. Ruiz, D. Cillero, P.J. Martínez, Á. Morales, G.S. Vicente, G. de Diego, J.M. Sánchez, Bench scale study of electrochemically promoted catalytic CO₂ hydrogenation to renewable fuels, *Catal. Today* 210 (2013) 55–66, <https://doi.org/10.1016/j.cattod.2012.10.025>.
- [59] A. de Lucas-Consuegra, J. González-Cobos, Y. García-Rodríguez, A. Mosquera, J. Endrino, J. Valverde, Enhancing the catalytic activity and selectivity of the partial oxidation of methanol by electrochemical promotion, *J. Catal.* 293 (2012) 149–157, <https://doi.org/10.1016/j.jcat.2012.06.016>.
- [60] M.P. Lavin-Lopez, A. Paton-Carrero, L. Sanchez-Silva, J.L. Valverde, A. Romero, Influence of the reduction strategy in the synthesis of reduced graphene oxide, *Adv. Powder Technol.* 28 (2017) 3195–3203, <https://doi.org/10.1016/j.apt.2017.09.032>.
- [61] D. Espinat, H. Dexpert, E. Freund, G. Martino, M. Couzi, P. Lespade, F. Cruege, Characterization of the coke formed on reforming catalysts by laser Raman spectroscopy, *Appl. Catal.* 16 (1985) 343–354, [https://doi.org/10.1016/S0166-9834\(00\)84398-5](https://doi.org/10.1016/S0166-9834(00)84398-5).
- [62] Y. Wang, D.C. Alsmeyer, R.L. McCreery, Raman spectroscopy of carbon materials: structural basis of observed spectra, *Chem. Mater.* 2 (1990) 557–563, <https://doi.org/10.1021/cm0ssss0011a018>.
- [63] J. Schwan, S. Ulrich, V. Batori, H. Ehrhardt, S. Silva, Raman spectroscopy on amorphous carbon films, *J. Appl. Phys.* 80 (1996) 440–447, <https://doi.org/10.1063/1.362745>.